



## Electrical Conductivity and Ion Exchange Properties of Polyaniline Antimony Tin Tungstate Nanocomposite

PREETHA B.

Department of Chemistry, Government College, Madappally, Vadakara,  
Kozhikode District, Kerala 673102, India.

\*Corresponding author E-mail: preethaba@gmail.com

<http://dx.doi.org/10.13005/ojc/370218>

(Received: February 10, 2021; Accepted: March 06, 2021)

### ABSTRACT

The nanocomposite, polyaniline antimony tin tungstate in the H<sup>+</sup> form was synthesized by a simple general method. EDS and ICP-AES methods were used to find the chemical constitution of the material. Further characterizations were done by TGA, XRD analysis, FTIR Spectroscopic analysis, UV-Visible DRS studies to find the optical properties, SEM for finding surface morphology, etc. Size determination using XRD peaks and TEM images confirmed its nano size. Investigation on ion exchange capacity and distribution coefficients for many metal ions revealed the ion exchange character. The composite exhibited differential selectivity for heavy metal ions such as Pb<sup>II</sup>, Th<sup>IV</sup>, Hg<sup>IV</sup>, etc. which are important in environmental applications like separation and treatment of polluted water from these metal ions. The electrical properties studied by Four-probe method revealed a high conductivity of 0.42 S/cm at room temperature and it decreases with an increase in temperature. These results suggest various applications of this nanocomposite in optoelectronics.

**Keywords;** Polyaniline, Antimony tin tungstate, Electrical conductivity, Ion exchange, Four probe.

### INTRODUCTION

Nanocomposites are multicomponent materials consisting of multiple phases in which at least one phase is continuous and have at least one dimension in the nanometer region. Their properties depend on various aspects, such as the nature of components including nanomaterial present, their composition, extent of distribution, size, shape, nanophase direction, interactions between different phases, pH, temperature, etc. Thus by selecting appropriate nanomaterials, nanocomposites of desired properties can be developed<sup>1</sup>. So the

synthesis and studies of new nanocomposites is very interesting and the present work is a study on the ion exchange properties and electrical properties of a novel nanocomposite synthesized from a conducting polymer and an inorganic cation exchanger.

Ion exchangers are materials having selectivity towards certain ions depending on various factors like the size of the ions, pore sizes, charge, structure etc. The synthesis of improved new inorganic ion exchangers has attracted the scientific world for the last few decades since they possess high thermal stability and ionizing radiation stability compared to



synthetic or natural organic ion exchangers available in the market. These inorganic ion exchangers find applications in nuclear industry, purification of metal ions, extracting valuable materials from industrial waste, separation of metal ions, hydrometallurgy, etc. Inorganic cation exchangers in their H<sup>+</sup> form possess protonic conduction. Scientists are interested in the development of new conducting organic polymers because of their high conductivity, stability, redox character, simple and economical method of synthesis. They find applications in photovoltaic cells, organic sensors etc. Among the group of conducting polymers, polyaniline is very important and much work has been done with functionalized polyaniline also<sup>2</sup> because simple chemical or electrochemical oxidative polymerisation method can be used for their synthesis and they possess ion exchange properties also. When a composite is synthesized with polyaniline and an inorganic ion exchanger, the properties will be improved due to their synergic interaction. The presence of polyaniline increases electrical conductivity. Thus newly developed nanocomposites with enhanced properties will be a promising new conducting material and can find application in water treatment, water softening, etc.<sup>1</sup>

Research on different ways of synthesis, detailed characterization and exploring the complete properties of conducting polymer composites are at the forefront of research in studying the mechanism of electron transport and in exploring their applications in divergent fields. Synthesis of new such systems will find great applications in environmental remediation due to their improved ion exchange properties and in electrical field due to their variability in conductivity and hence the reversibility to their insulating and conducting forms<sup>2</sup>. A review of some of the nanocomposites of this class shows how the properties are improved from that of their components.

The electrical conductivity of the composite, polyaniline Sn(IV) tungstophosphate, reported was found to be semiconducting and the value was very high compared to that of pure polyaniline in addition to its ion-exchange properties<sup>3</sup>. Similarly, the electrical conductivity and Pb(II) selectivity on polyaniline Sn(IV) tungstomolybdate nanocomposite and its use as membrane electrodes were thoroughly investigated by Zeid Abdullah AlOthman *et al.*,<sup>4</sup> and the electrical conductivity was found in the

semiconductor region; i.e., 10<sup>-2</sup> Scm<sup>-1</sup> which is also higher than that of pure polyaniline.

Similarly, polythiophene was inserted into tin(IV) phosphate to synthesize polythiophene tin(IV) phosphate and the works on it revealed that the conductivity and ion exchange of heavy metal ions enhanced. The conductivity determined was 4.0 × 10<sup>-2</sup>–1.0 × 10<sup>-3</sup> S/cm<sup>5</sup>.

Studies on the electrical conductivity of polypyrrole–zirconium(IV) phosphate nanocomposite showed that it possessed high ion-exchange capacity of 1.60 meqg<sup>-1</sup> and electrical conductivity value of 0.33 Scm<sup>-1</sup> and isothermal stability of electrical conductivity up to 100°C. Ammonia vapor sensing performance of it was also explored<sup>6</sup>. Properties of the above-reported nanocomposites revealed that these possessed improved properties compared to their individual components.

Synthesis and properties of tin tungstate and antimony tungstate ion exchangers were reported earlier. They possessed high ion exchange capacity and found good applications in separating and removing metal ions from aqueous medium<sup>7,8</sup>. Ion-exchange character and electrical conductivity of polyaniline synthesized by various methods were also reported<sup>9-11</sup>. But a composite of these has not been reported so far and hence in this study, we synthesized antimony tin tungstate as the inorganic part and polyaniline is incorporated into the matrices to get a nanocomposite of improved properties.

## MATERIALS AND METHODS

For the synthesis and studies of the material, analytical reagents and chemicals were used. The chemicals used were of LOBA make. pH measurements were done using ELICO LI613 pH meter and for heating the sample an electric thermostat oven was used. Optical studies were carried out using the UV-Visible Spectrophotometer of JASCO V660 make with an integrated sphere attachment. FTIR Spectrometer of Thermo-Nicolet Avtar 370 make for IR studies, X-ray Diffractometer Bruker AXS D8 Advance for XRD studies, Perkin Elmer Diamond TG/DTA analysis system for thermal analysis were also used. The SEM-EDX analyses were carried out with the help of a computer-controlled field emission SEM (JEOL JSM-6330F,

JEOL Ltd., Akishima Tokyo 196-8558 Japan). TEM analysis was done using FEI Tecnai G2 30 S-TWIN with voltage acceleration of 100 kV. The electrical conductivity of the composite was determined by the Four-probe method. Conductivity studies were carried out at various temperatures from 40°C to 100°C using a Keithley high voltage current source and low noise multimeter.

### Synthesis

#### Polyaniline

Polymerization of aniline was carried out in aqueous solution at 10°C. For this, a 10% solution of aniline in 0.1 M HCl was used. The oxidative polymerization of aniline was initiated by the dropwise addition of 0.1M aqueous ammonium persulphate in 0.1 M HCl solution. Rate of addition was controlled to meet the exothermic character of reaction. The pH of the solution was maintained at 3 to get the emeraldine form of polyaniline. The mixture was stirred for 1 h at 10°C on a magnetic stirrer for complete polymerization. The color of the resin first obtained was bluish-green which changed to green due to the formation of emeraldine salt.

#### Antimony tin tungstate sol

It was prepared by adding 0.1 M sodium tungstate solution to a mixture of 0.1 M solutions of antimony trichloride and stannic chloride in the ratio 1:1:4 by volume with constant stirring.

#### Polyaniline antimony tin tungstate (PANI Sb-Sn-W)

The polyaniline sol synthesized as above was added dropwise to the antimony tin tungstate sol with constant stirring. It was allowed to remain for 24 h at normal temperature maintaining the pH at 2, filtered, washed and dried. 1.0 M nitric acid was used for converting it into H<sup>+</sup> form. It was then washed, allowed to dry and particles of consistent sizes were separated.

#### Characterization

Ion exchange capacity which is a magnitude of the exchangeable protons present in the material was estimated by eluting the protons in the material by alkali metal chloride like sodium chloride to pass through the ion exchanger taken in a column and is usually expressed as milliequivalents per gram of exchanger<sup>12</sup>.

The distribution coefficient ( $k_d$ ) is the fraction of concentration of metal ion on the solid part to concentration of that ion in the liquid at equilibrium. The distribution coefficients of different metal ions were found out by keeping 0.1 g of the exchanger in equilibrium with 20 mL of various 0.005M metal ion solutions for one day at atmospheric temperature. Complexometric titration methods and spectrophotometric methods were used to find the concentrations of metal ions before and after equilibrium. From these,  $K_d$  was calculated as

$$k_d = \frac{\text{milliequivalents of ion per g of exchanger}}{\text{milliequivalents of ion per ml of solution}} \quad 12$$

XRD study helped to find the average size of particles using the Debye-Scherrer equation,  $D = \frac{0.9\lambda}{\beta_{2\theta} \cos\theta_{\max}}$  where D is the average crystal size in nm,  $\lambda$  is the wavelength of X-ray,  $\theta$  is the diffraction angle of the X-ray and  $\beta_{2\theta}$  is FWHM of a peak<sup>13</sup>. The X-ray generator was operated at 35 kV and 30mA using Copper K $\alpha$  ( $\lambda=1.5418\text{\AA}$ ) as source of radiation. The intensity values were taken for  $2\theta$  values up to 60° with a 0.01° step and with a counting time of 0.2s/point.

Scanning electron microscopy (SEM) helped to study the surface morphology. When it is used along with electron dispersive spectroscopy (EDS), composition of various elements on microscopic portions of the nanocomposite can be found and it is also used to find whether any contaminants are present. EDS is a technique that utilizes X-rays emitted from the sample after it is bombarded by the electron beam to identify the elemental ratio in the sample. ICP-AES analysis technique was also used to confirm the composition.

TEM is capable of imaging at a significantly higher resolution than SEM. The size was determined from the image which confirmed the nanosize.

#### Fourier Transform Infrared (FTIR) Spectroscopy

IR spectrum can be used for the determination of groups, free water molecules, metal-oxygen stretching, etc. The frequencies were noted as wave numbers mainly over the range of 4000cm<sup>-1</sup> – 400cm<sup>-1</sup>. Spectrum is obtained due to the bond vibration frequencies which indicate the presence of various types of bonds and functional groups in the material.

### Thermal analysis

Certain characteristics of the material such as adsorbed water, water of hydration, stability of the substance, etc. are obtained from the thermal studies. The samples were heated at a rate of 20°C/min in the range of 40°C to 1030°C and the nitrogen flow rate was kept at 20ml/minute.

### UV-Visible Diffuse Reflectance Spectroscopy

In a DRS, the ratio of the intensities of lights scattered from a sample of thickness 3 mm and a completely reflecting reference sample is determined as a function of wavelength. DRS is widely used to study transition metal oxides for getting information on surface coordination and various oxidation states of metal ions by studying d-d, f-d transitions and oxygen - metal ion charge transfer bands.

### Electrical conductivity by Four-Probe Method

Four probe apparatus is used for the determination of conductivity of semiconductors. It is also used for the measurement of conductivity in materials possessing different shapes. Using this 4-in-line-probe dc conductivity measuring equipment, current-voltage data can be obtained. Using the data at various temperatures we can study the conductivity and its mechanism. In the equipment there is an oven provided with a heater so that we can heat the sample and the conducting behavior is studied by increasing the temperature from 40°C to 100°C.

## RESULTS AND DISCUSSION

The polymerization of aniline in aqueous solution proceeded on the addition of ammonium persulphate and PANI emeraldine salt is formed which is confirmed with a color change from blue to dark green<sup>14</sup>. The color change is due to the formation of polyaniline in different oxidation states. This property of polyaniline find applications in sensors and electrochromic appliances. These sensors work on the principle of variation in electrical conductivity with different oxidation states or extent of doping. The inorganic ion exchanger, antimony tin tungstate synthesized was made a composite with the polyaniline. The synthesized polyaniline antimony tin tungstate (PANI SbSnW) possessed the synergic effect of the electrical, redox and ion exchange properties of single components. Ionic interaction causes the binding of polyaniline into the matrix of antimony tin tungstate<sup>1</sup>.

The SEM images (Fig.1) of the material in different magnifications showed that the material consisted of large agglomerates. The particles are in nanosize with a high surface area.

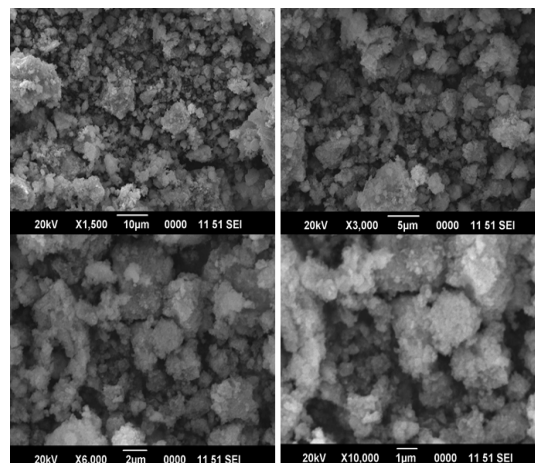


Fig. 1. SEM images of PANI SbSnW

### EDS for elemental composition

When the composite was bombarded with a beam of electrons by SEM, electrons from the atoms present on the surface of the composite were ejected. These vacancies produced as a result of electron ejection were filled by the jumping of electrons from a higher energy level and the energy difference between the two levels were emitted as X-rays. These energies of the X-rays are characteristic of the elements on the surface of the composite. So if an EDS X-ray detector is attached with a SEM it determines the intensity of X-rays emitted against the characteristic energies of elements. Detector used was lithium-drifted silicon solid-state device. Corresponding to the energy of the X-rays, a charge pulse was created when the X-ray emitted from the surface of the composite fell on the EDS detector. A voltage pulse generated corresponding to this charging pulse. A multichannel analyzer sorted these pulse signals according to the voltage. The voltage corresponding to each X-ray energy was determined and these were sent to a computer for further data processing. Thus the elemental composition at the surface of the composite was determined. The EDS patterns showed the presence of N, Sb, Sn, W, and O without any major impurity. The composition of N, Sb, Sn, W, and O was found to be 1: 1: 2: 5.

As the TEM analysis provides more resolution than SEM, further analysis of size was done using TEM. In this, an electron beam from an

electron gun was focused on a small and thin surface of the composite by using a lens which helps to condense. The thickness and electron transparency of the specimen determines the transmittance of the electron beam striking on the surface. An image is created by these transmitted electrons when focused by the objective lens. This TEM image was further magnified in the instrument. This again struck the phosphor screen where light was produced so that it would be visible. The dark areas of the image showed that the electrons transmitted through this sample area are less. The bright areas of the image showed areas of the sample from where more electrons were transmitted. TEM analysis confirmed the size of the composite in the nano region (Fig. 2). The particles were found to be agglomerated.

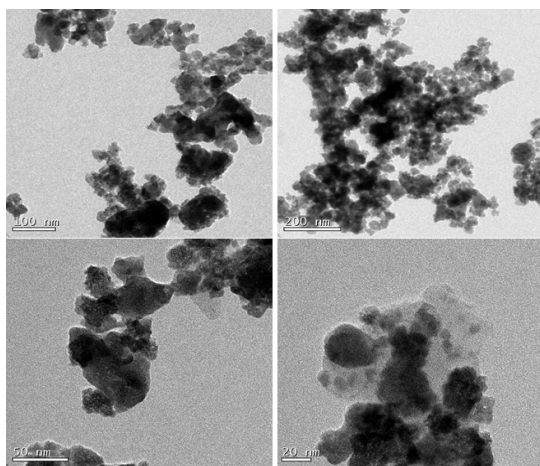


Fig. 2. TEM images of PANISbSnW

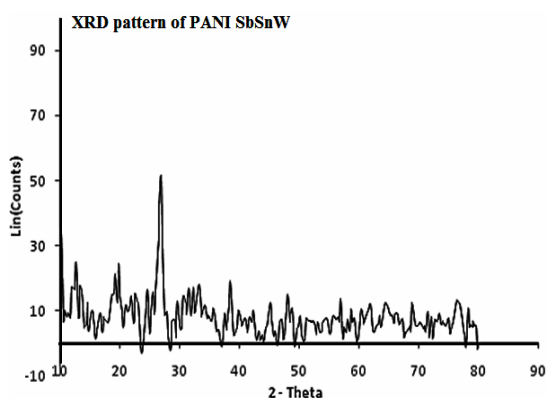


Fig. 3. XRD pattern of PANISbSnW

The position and intensity of the diffraction peaks in an X-ray scattering pattern show the crystal structure of a sample. Inter atomic distances can be known from the positions of the diffraction peaks. The diffraction peak intensities reveal the atom types and

positions. XRD analysis (Fig. 3) of the composite showed the amorphous nature of the exchanger as there was only one intense peak. Debye-Scherrer equation was used to determine the particle size by noting the full width at half-maximum of the most intense peak in the XRD. The average particle size calculated was found to be 38 nm, confirming the nano size.

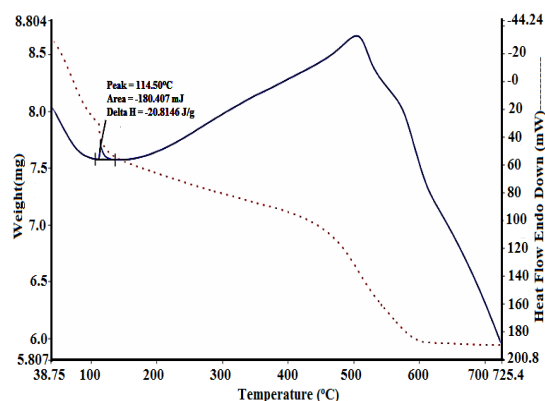


Fig. 4. Thermal analysis diagrams of PANISbSnW

Based on enthalpy changes associated with the chemical reactions occurring, quantitative measurements can be carried out. Thermal data (Fig. 4) showed the evaporation of free water molecules as seen from the initial weight loss of 5% up to 114°C which was accompanied by an endotherm. A gradual weight loss of about 27% was shown up to about 450°C. This can be explained as due to the condensation of hydroxyl groups present in the structure. The material showed stability up to about 450°C.

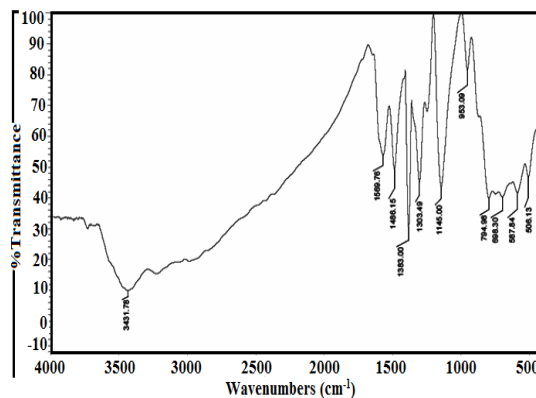
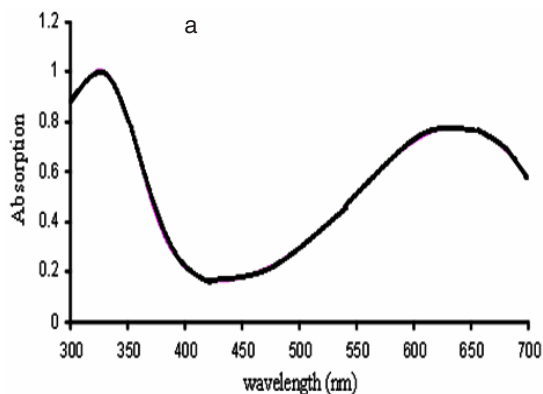


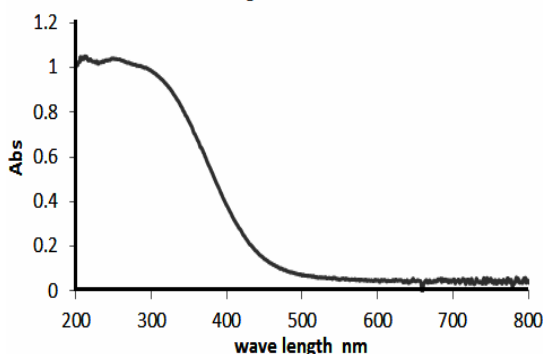
Fig. 5. FTIR spectrum of PANISbSnW

FTIR spectrum of PANISbSnW (Fig. 5) showed a wide band at around 3430  $\text{cm}^{-1}$  due to symmetric and asymmetric O-H stretching vibration. The band at  $\sim 1570 \text{ cm}^{-1}$  can be due to H-O-H bending vibration. The spectrum confirmed the presence of exchangeable protons which is essential for cation

exchangers. C–N bond vibrations at  $1303\text{ cm}^{-1}$ , C=C bond vibrations at  $1486\text{ cm}^{-1}$ , and C–H vibrations at  $1145\text{ cm}^{-1}$  were also observed<sup>15</sup>. Various vibrations in the FTIR spectrum confirmed the material as PANISbSnW.



b. UV-Vis spectrum of SbSnW



c. UV Vis Spectrum of PANI SbSnW

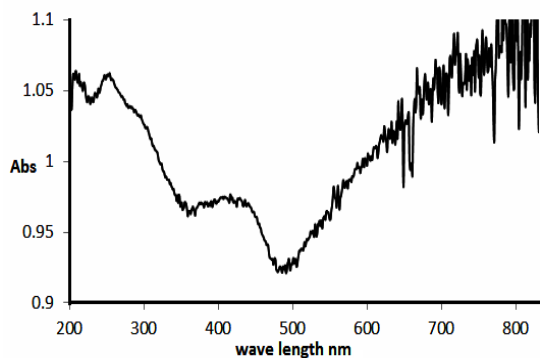


Fig. 6. UV-Vis spectra of (a) Polyaniline (PANI)<sup>16</sup> (b) SbSnW (c) PANI SbSnW

UV-Vis spectroscopic studies revealed that the peak around 305 nm arises from  $\pi$ - $\pi^*$  electron transition within the benzoid ring. The band at about 420 nm is due to  $\pi$ -polaron transitions confirming the formation of protonated emeraldine<sup>17</sup>. Polarons are the charge carriers. This shoulder is also present

in pure antimony tin tungstate corresponding to the band gap energy. Groups in PANI such as =NH and inorganic part is a conductor. This combination enhanced electron mobility in the composite<sup>18</sup>.

The rising portion above 700 nm corresponds to the  $\pi$ -polaron transition. The peak around 800 nm indicated a compact tightly coiled chain conformation of PANI which confirmed the presence of conducting PANI. The free-carrier tail starting from 800 nm to the IR region showed high conductivity of the material. Conductivity was in the region characteristic of the conductivity of metals<sup>19</sup>.

When the inorganic nanoparticles were inserted in the PANI, a major change was observed in the absorbance. The shift of the absorption transition to higher wavelength may be due to the interaction of metal nanoparticles with the organic polymer<sup>20</sup>.

The doping level can be estimated from the UV Diffuse Reflectance spectrum by determining the exciton ( $\pi$ -polaron transition) - benzenoid ( $\pi$ - $\pi^*$  transition) ratio<sup>21</sup>. In the spectrum of pure antimony tin tungstate no peaks were found above 500 nm. PANI SbSnW composite showed good similarity in their UV-Vis spectrum with that of PANI reported earlier<sup>16</sup>, particularly with the presence of the absorption around 420 nm and 500 nm which are associated with the stabilization of the composite in the emeraldine form<sup>22</sup>. A comparison of the PANI and PANI SbSnW composite spectra showed that SbSnW stabilized the polyaniline in its emeraldine form.

The ion exchange capacity of the composite with sodium ions was found to be 1.37 meq/g revealing that it possessed exchangeable protons. Appreciable loss in ion exchange capacity was not noticed even after the regeneration of the ion exchanger thrice. The stability of the composite in various acids and alkalis was tested. For this, 0.5 g of samples were kept in 50 mL of different reagents for 24 h and changes in color, nature and weight of the samples were observed and found that the material was quite stable in 1.0 M acids and in 0.01 M bases.

The ion exchange capacity decreases (Table 1) slowly with temperature and the sample possessed exchange capacity up to 300°C. Studies on these were carried out by determining the ion exchange capacities after keeping the material

at various temperatures in an electric oven for three hours each. The obtained thermogram revealed a decrease in ion exchange capacity with temperature.

**Table 1: Effect of temperature on IEC**

Temperature °C	Duration (h)	IEC
50	3	1.37
100	3	1.23
150	3	1.08
200	3	0.96
300	3	0.81
400	3	0.77

Selectivity is a characteristic property of an ion exchanger, which makes the exchanger prefer one counter ion to another. Distribution studies of metal ions (Fig. 7) revealed the selectivity of the composite. It showed a very high affinity towards  $Pb^{2+}$ ,  $Th^{4+}$ ,  $Hg^{2+}$ , etc. The selectivity was found to be in the order  $Pb^{2+} > Th^{4+} > Hg^{2+} > Al^{3+} > Mn^{2+} > Cu^{2+} > Cd^{2+} > Ni^{2+} > Mg > Co^{2+}$ . The results showed the application of the nanocomposite for separating various metal ions and also for removing heavy metal ions from polluted water. The rate at which two constituents separate in the ion exchange column is determined as the ratio of the two corresponding distribution coefficients and this ratio is called separation factor. This separation factor,  $\alpha$  is used as a measure of the extent of separation possible in chromatography.  $\alpha = k_{d1}/k_{d2}$ , where  $k_{d1}$  and  $k_{d2}$  are the distribution coefficients of the two metal ions in solution. The separation will be easier if  $\alpha$  deviates greatly from unity. Hence using this newly synthesized nanocomposite, separation of Pb(II) from other ions can be carried out easily since the separation factor is more than 2.

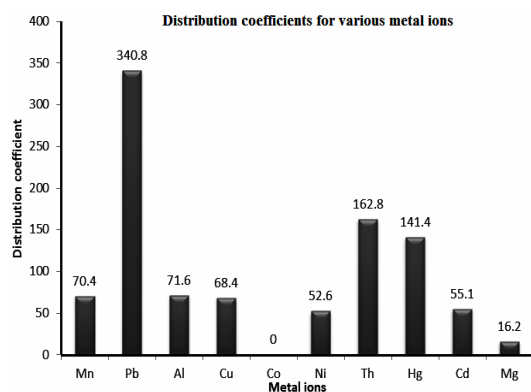


**Fig. 7. Distribution coefficients of various metal ions**

The composite possessed prominent ion exchange capacity at increased temperatures and high-temperature applications can be explored. It was well characterized for their ion-exchange properties and found to be chemically and thermally stable. It showed differential selectivity to metal ions. Due to the nano size, it possessed a high surface area which improves its catalytic activity. Also it possessed UV-absorption capability as revealed from the UV-Vis Diffuse Reflectance studies. This property can be used to filter UV-light.

For electrical conductivity measurement, the sample was made in pellet form of 13mm diameter and 1mm thickness at a pressure of 14 Mpa. A Carver model C Press was used for this. The conductivity of the PANISbSnW nanocomposite was determined by Four Probe method. The variations of electrical conductivity of the composite with increasing temperatures were thoroughly investigated.

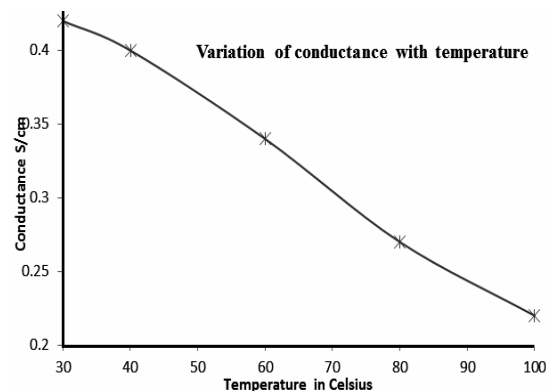


**Fig. 8. Variation of electrical conductivity with temperature**

The electrical conductivity of organic polymers is due to the presence of conjugated double bonds in the backbone. The mechanism of conduction in these polymers can be understood using the concept of polaron and bipolaron. Low level oxidation of the polymer gives polaron and higher level oxidation gives bipolaron. Polarons and bipolarons move along the polymer backbone by the interchange of single and double bonds in the conjugated chain. In the case of inorganic ion exchangers, they possess protonic conduction.

Studies by using the Four-Probe method revealed that the conductivity of PANI SbSnW was

very high compared to that of polyaniline and most of the polyaniline composites synthesized by incorporating similar inorganic components. The properties of the nanocomposite enhanced due to the synergic effect of the organic and inorganic part. The electrical conductivities of the material decreased with increase of temperature (Fig. 8) and the values were in the range of  $4.2 - 2 \times 10^{-1} \text{ Scm}^{-1}$  which lies on the border of the semiconductor and conductor region. The electrical conductivities were determined against time at ambient temperatures, 40, 60, 80, and 100°C which showed stability in conductivity with time. The rate of decrease in conductivity is high up to 80°C. After that, the rate of decrease was less. This is because at the initial stages there was protonic conduction (due to the inorganic ion exchanger part) also. As temperature increases protonic conduction decreases and at the later part there will be conduction due to the organic polymeric part only. PANI has great contribution in the electron transport mechanisms of nanocomposites. The conductivity of the nanocomposite depends upon the degree of oxidation and degree of protonation of polyaniline as well as the protonic conduction of the inorganic part.

The presence of protons in the structural hydroxyl groups in the composite indicates promising applications in eco-friendly solid acid catalysis. Compared to other polymer nanocomposites reported, this study explores its promising applications in various other fields.

## CONCLUSION

The nanocomposite, polyaniline antimony tin tungstate studied was synthesized by an eco-friendly method followed by conversion into the  $\text{H}^+$  form. Interesting information on the physicochemical characteristics of the material was obtained using various analytical and spectroscopic methods. Studies revealed that this material is a good solid acid catalyst. The material showed very high stability. The introduction of organic species has enhanced the properties of the inorganic ion exchanger. It possessed high selectivity for heavy metal ions like  $\text{Pb}^{2+}$ ,  $\text{Th}^{4+}$ ,  $\text{Hg}^{2+}$ , etc. These results contribute much in environmental chemistry and can be utilized for applications in separation and removal of these metal ions<sup>23</sup>.

Studies on electrical properties using Four – probe method showed that the composite possessed prominent conductivity at room temperature and it decreases with temperature.<sup>24</sup> These results suggest that the composite is very promising and can find various applications in optoelectronics in addition to its ion exchange applications.

## ACKNOWLEDGMENT

The author thank KSCSTE, Kerala for providing financial assistance 28/SPS 58/2016/KSCSTE for the project work.

## Conflicts of Interest

The authors declare no conflict of interest.

## REFERENCES

- Jacynth Mispa, P.; Subramaniam, P.; Murugesan, R. *J. Polym.*, **2013**, 7, 1-12.
- Gyorgy Inzelt. *Conducting Polymers: A New Era In Electrochemistry*, Springer., **2008**, 4.
- Nabi, S.A.; ArshiaAkhtar; Md. Dilwar Alam; KhanMeraj AlamKhan *Desalination.*, **2014**, 340(1), 73-83.
- Zeid Abdullah ALOthman.; Mohammad Mezbaul Alam.; Mu. Naushad.; Rani Bushra *Int. J. Electrochem. Sci.*, **2015**, 10, 2663 -2684
- AnishKhan.; Abdullah M. Asiri.; Aftab Aslam Parwaz.; Khan Sher Bahadar Khan, *Arab. J. Chem.*, **2019**, 12, 1652-1659.
- Asif Ali Khan.; Rizwan Hussain.; Umair Baig, *Int. J. Ind. Chem.*, **2017**, 8, 157–173.
- Manoj Sadanandan.; Beena Raveendran *Bull. Chem. React. Eng. Catal.*, **2012**, 7(2), 105-111
- Janardanan, C.; Nair, S. M. K.; *Indian J. Chem.*, **1992**, 31A, 136.
- Suganthi, R.; Padmaja S.; Jhancy Mary, S.; *Asian J. Chem.*, **2020**, 32(2), 265-270.
- Shoba, E.; Pasupathy, N.; Thirunavukkarasu, P.; Chandrasekaran, J.; Parthasarathy, G. *Asian J. Chem.*, **2019**, 31(2), 2846-2854.



11. Deepa, N. A.; Dhivya, C.; Anbu Anjugam Vandarkuzhali, S.; Santhi R.; Radha, N. *Asian J. Chem.*, **2014**, *26*(15), 4855-4864.
12. Vogel, A. I. "A textbook of Quantitative Inorganic Analysis", Longman Group Limited, London., **1975**.
13. Hasliza Bahruji.; Michael Bowker.; Philip R. Davies *J. Chem. Sci.*, **2019**, *131*(33), 1-7.
14. Syed Shahabuddin.; Norazilawati Muhamad Sarih.; Muhammad Afzal Kamboh.; Hamid Rashidi Nodeh.; *Sharifah Mohamad Polymers.*, **2016**, *8*(9), 1-19.
15. Bogdan Butoi.; Andreea Groza.; Paul Dinca.; Adriana Balan.; *Valentin Barna Polymers.*, **2017**, *9*, 732.
16. Jacek Niziol.; Maciek Sniechowski.; Anna Podraza-Guba.; Jan Pielichowski.; *Polym. Bull.*, **2011**, *66*, 761-770.
17. Arup Choudhury *Sens, Actuator, B.*, **2009**, *138*, 318-325.
18. Anish Khan.; Abdullah M. Asiri Aftab Aslam Parwaz Khan.; Sher Bahadar Khan, *Arab. J. Chem.*, **2009**, *12*, 1652-1659.
19. Sudha, J. D.; Sivakala, S. *Colloid. Polym. Sci.*, **2009**, *287*, 1347.
20. Manawwer Alam.; Anees A. Ansari.; Mohammed Rafi Shaik.; Naser M. Alandis, *Arab. J. Chem.*, **2013**, *6*(3), 341-345.
21. Anwar-ul-Haq Ali Shah.; Muhammad Kamran.; Salma Bilal.; Rizwan Ullah, *Materials.*, **2019**, *12*, 1527.
22. Vaishali Kamblea.; Gunjan Kodwania.; Ramdoss Sridharkrishna.; Balaprasad Ankamwar, *Adv. Nano. Res.*, **2014**, *2*, 111-119.
23. Harinath Yapati.; Sreenu Bhogineni.; Suresh Chirumamilla.; Seshaiyah, K. *J. Chem. Sci.*, **2016**, *128*, 779-786.
24. Ram Krishna Hona.; Farshid Ramezanipour *J. Chem. Sci.*, **2019**, *131*(109), 1-18.